



Article

# Biocomposites Produced from Hardwood Particles by Equal Channel Angular Pressing: Effects of Pre-Treatment

Yu Bai <sup>1,\*</sup>, Xiaoqing Zhang <sup>2</sup> and Kenong Xia <sup>1,\*</sup> 

<sup>1</sup> Department of Mechanical Engineering, The University of Melbourne, Parkville, VIC 3010, Australia

<sup>2</sup> CSIRO Manufacturing, Private Bag 10, Clayton South, VIC 3169, Australia; Xiaoqing.Zhang@csiro.au

\* Correspondence: ybai1@student.unimelb.edu.au (Y.B.); k.xia@unimelb.edu.au (K.X.)

Received: 20 November 2020; Accepted: 27 November 2020; Published: 30 November 2020



**Abstract:** The benefit of using a combination of alkali pre-treatment and ball milling in processing hardwood particles into biocomposites via equal channel angular pressing (ECAP) was demonstrated. The penetration of bonding additives (polyethyleneimine and tannic acid) into hardwood structures was enhanced by the pre-treatment, resulting in plasticization and cross-linking derived from the additives during the particle processing. A significant improvement in the biocomposites' mechanical properties was obtained, reaching flexural strength of 28–29 MPa and flexural modulus of 3650 MPa, comparable to those displayed by commercial wood fiberboard using thermosetting resins as the binding agent. This adds to the promise of developing biocomposites from industrial or agricultural waste through the simple and efficient ECAP technology in conjunction with common pre-treatment methodologies for wood particles.

**Keywords:** biocomposites; particle processing; consolidation; mechanical properties

## 1. Introduction

During the last 2–3 decades, a rapid expansion of scientific research has been occurring in developing bio-based materials to address environmental issues caused by using plastics produced from fossil resources such as petroleum and natural gas [1]. Because of the non-renewable, slow-degradable, or non-biodegradable nature of those plastic materials, the solid waste has contributed to the significant accumulations in landfills and pollution in oceans [1]. The enormous carbon footprint associated with the plastic life cycle is represented by a large amount of carbon dioxide rapidly released into the environment [1,2]. Although some plastics such as polypropylene (PP) and polyethylene (PE) can be recycled and reused [3], the detrimental environmental impact has been well recognized, and exploring bio-based polymers from renewable biomass feedstocks is considered as a long-term alternative [1].

To develop bio-based materials from agricultural or industrial biomass waste via effective processing has been a challenging objective. Lignocellulose is the most abundant biomass in nature with excellent properties in many aspects [4,5]. Utilizing it from waste streams to generate renewable and biodegradable materials would greatly benefit both economics and the environment without competing with agricultural products' food and energy consumption. Wood chips/fibers/powders have been commercially used in fabricating particleboard and medium-density fiberboard using thermoset resins as binder mainly by compression molding. Thermal extrusion, injection molding, or thermal forming can also be used to produce wood-plastic composites when a thermoplastic polymer is used as a continuous matrix, and the thermal processability relies on melting the thermoplastic. It would be limited by lignocellulose's thermal properties, which would experience thermal decomposition before melting [6]. There are also difficulties in effective and efficient plasticization, deformation, and lignocellulose processing associated with cellulose's highly crystalline structure [7,8].

We have demonstrated that equal channel angular pressing (ECAP) is a new promising methodology to process bio-based polymer powders into bulk materials at relatively low temperatures [9,10]. The high shear deformation during ECAP could effectively consolidate cellulose and wood particles at ~200 °C directly into biocomposites with continuous morphologies in full density [10–12]. When using a small amount of plasticizing/cross-linking additives such as PEI (polyethyleneimine) in the ECAP processing of wood particles, the biocomposites' processability and binding performance were significantly improved [13]. However, cracking did occur under the high shear deformation condition during ECAP. Therefore, the processing conditions need to be optimized, and some level of surface modification of the wood particles may be desirable through pre-treatment to enhance the binding performance to mitigate the risk of crack formation.

This paper reports our recent results using common pre-treatment methodologies to modify the surface of wood particles for improving processing performance and properties of the obtained biocomposites. In addition, tannic acid (TA) was applied in conjunction with PEI to boost cross-linking via the formation of covalent bonds or hydrogen bonding between TA and cellulose/lignin for improving mechanical properties. The microstructures, intermolecular interactions between various components, mechanical properties, and thermal stability of the biocomposites were investigated and correlated in order to achieve a good understanding of the relationship between processing conditions and material structures/properties.

## 2. Materials and Methods

The maple (*Acer spp.*) hardwood (HW) particles from American Wood Fibers (Schofield, WI, USA) and highly branched polyethyleneimine (PEI) (with average molecular weights of  $M_n \sim 600$  g/mol and  $M_w \sim 800$  g/mol) from Sigma-Aldrich (Saint Louis, MO, USA) used in this work were the same as those previously reported [13]. Tannic acid (TA, CAS Number 1401-55-4) was purchased from Sigma-Aldrich (Saint Louis, MO, USA).

The alkali pre-treatment was performed by soaking HW particles in a low concentration sodium hydroxide (NaOH) aqueous solution (pH = 10) at room temperature for 5 h. The treated HW particles were then filtered and dried in an oven at 60 °C for over 24 h.

Ball milling (planetary) of HW particles was conducted at 300 rpm for 2 h (with a 12 min break after the first hour). The weight ratio of HW particles to steel balls was 1:20, while the weight ratio of large to small (10 and 6 mm in diameter, respectively) steel balls was 1:1. The pre-treated HW with their simplified identities is displayed in Table 1.

**Table 1.** Hardwood (HW) without or with binder (PEI or PEI/TA) using different pre-treatments.

Composition in wt%	Identification
Alkali treated HW	HW:A
2h-ball milled HW	HW:M
Alkali treated + 2h-ball milled HW	HW:(A + M)
HW/PEI = 90/10	HW/PEI
HW/PEI/TA = 86/11/3	HW/PEI/TA
Alkali treated HW/PEI = 90/10	HW/PEI:A
Alkali treated HW/PEI/TA = 86/11/3	HW/PEI/TA:A
2h-ball milled HW/PEI = 90/10	HW/PEI:M
2h-ball milled HW/PEI/TA = 86/11/3	HW/PEI/TA:M
Alkali treated + 2h-ball milled HW/PEI = 90/10	HW/PEI:(A + M)
Alkali treated + 2h-ball milled HW/PEI/TA = 86/11/3	HW/PEI/TA:(A + M)

For the preparation of HW/PEI, a PEI solution (28 wt% in water) was added to HW particles to achieve HW/PEI = 90/10 in wt% after drying. When preparing HW/PEI/TA, PEI and TA were dissolved separately in water to make 45 wt% and 19 wt% solutions, respectively. The two solutions were added to HW to obtain HW/PEI/TA = 86/11/3 in wt% after drying. The mixture was thoroughly mixed at

room temperature and then dried at 60 °C for over 24 h. These samples with their simplified identities are also listed in Table 1.

The ECAP set-up was the same as in the previous work [9], with two channels of equal cross-section (9 × 9 mm) intersecting at 90°. Polytetrafluoroethylene (PTFE) lubricant coating was applied to the channel walls to reduce the friction at the channel walls. The HW/binder mixtures were pressed at a constant speed of 25 mm/min and temperature of 200 °C (controlled to ±2 °C) with a back pressure of ~100 MPa, resulting in consolidated samples of 40–50 mm in length.

Wood particles embedded in epoxy resin and the longitudinal sections of the consolidated samples were ground using silicon carbide paper to prepare the surfaces for microstructure observation and polished using diamond paste (3 μm). These samples were used for observation by optical microscopy (Olympus BH2-UMA, Tokyo, Japan), fluorescence microscopy (Leica M205A, Wetzlar, Germany) with three filters—DAPI, GFP1, and mCherry, and scanning electron microscopy (SEM, FEI Quanta 200 ESEM FEG, Waltham, MA, USA).

A Thermo Fisher Scientific Nicolet 6700 FT-IR Spectrometer was used to characterize the molecular vibration of the functional groups of the HW samples over a scan range of 600–4000 cm<sup>-1</sup> at a resolution of 4 cm<sup>-1</sup>. The baselines of these spectra were subtracted, followed by vector normalization for comparison.

Three-point bending tests for the consolidated specimens were conducted using the 810 Material Test System, with a lower support span of 32 mm at a crosshead speed of 1 mm/min until fracture, after pre-conditioning at room temperature under a relative humidity of 50 ± 2% for over 24 h. Dynamic mechanical analysis (DMA) or thermogravimetric analysis (TGA) were conducted on a PerkinElmer PYRIS Diamond DMA (Waltham, MA, USA) or Mettler Toledo TGA/SDTA851<sup>e</sup> (Greifensee, Switzerland) under conditions described in a previous paper [13].

### 3. Results and Discussion

#### 3.1. Microstructures

Optical microstructures of HW particles after different pre-treatments are shown in Figure 1. As expected, alkali treatment did not cause much change in particle size. In contrast, ball milling had caused the generation of a large amount of HW fines. At higher magnification (Figure 2), the undeformed wood cells in HW with open lumina of vessels (arrows in Figure 2a) were converted to collapsed vessels (arrows in Figure 2b) after ball milling. SEM confirmed the collapse of wood cells (Figure 3). The fine particles generated by ball milling appeared to contain highly distorted cells that were more continuous than distinctive, as shown in Figure 3c.

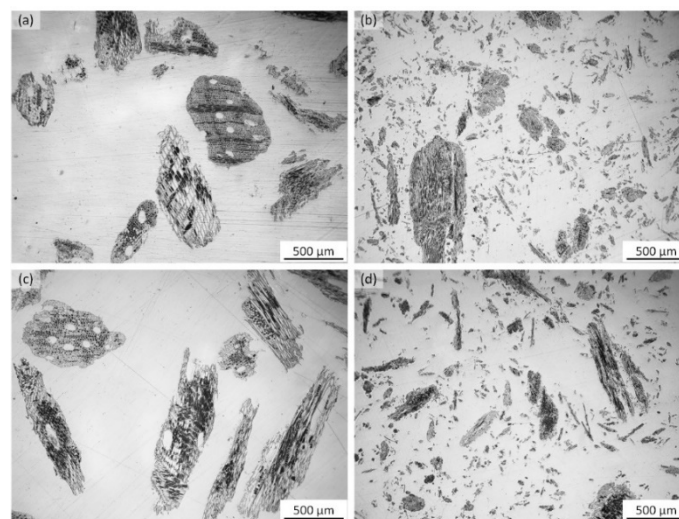


**Figure 1.** Optical microstructures of: (a) HW, (b) HW:M, (c) HW:A and (d) HW:(A + M).

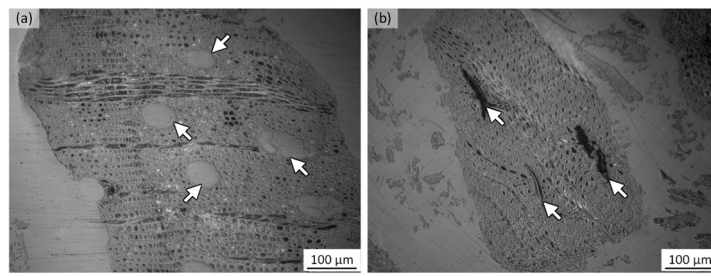


**Figure 2.** Optical microstructures of (a) HW and (b) HW:M with white arrows pointing to vessels.

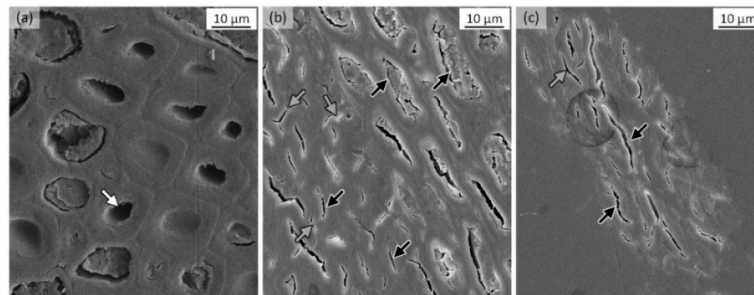


**Figure 3.** SEM microstructures of (a) HW showing undeformed wood cells, with a white arrow pointing to a lumen; (b) large particle and (c) fine particle in HW:M, with black arrows pointing to lumen gaps of fully or partially collapsed wood cells and grey arrows to cracks at middle lamella causing separation of cell walls.

After ECAP, consolidated bulk composites were obtained, as shown in Figure 4, in conjunction with their optical microstructures. It is noted that the particles tended to orient along the pressing direction, and no cracking or severe shearing was observed in most of the sample volume. However, there were periodic regions where either cracks (black arrows) or shear bands (between dashed lines) along the shear direction ( $\sim 45^\circ$  relative to the pressing direction) were present. The cracks were usually observed in the samples without ball milling (Figure 4a–d), with surrounding particles aligning at higher angles (up to  $40^\circ$ ). By contrast, the shear bands were found typically in the samples with ball milling (Figure 4e–h), with the surrounding particles appearing to orient at slightly lower angles (up to  $30^\circ$ ). The SEM microstructures in Figure 5 show cracks along the ECAP shear direction passing through less deformed or largely distorted cells in HW/PEI/TA and HW/PEI:(A + M). Cracks were sometimes seen to be surrounded by distorted cell structures (Figure 5c,f) with fibril pull-out (grey arrow in Figure 5f).

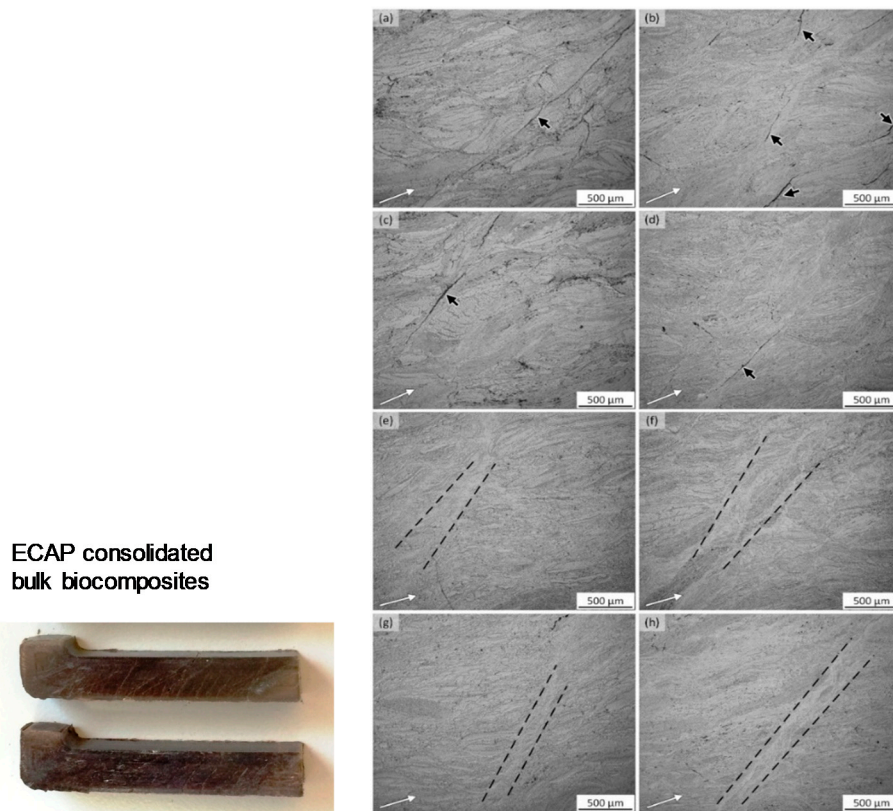


**Figure 4.** Typical equal channel angular pressing (ECAP) consolidated samples (left) and their optical images of microstructures showing regions with cracks (black arrows) in (a) HW/PEI, (b) HW/PEI/TA, (c) HW/PEI:A, (d) HW/PEI/TA:A, and shear bands (between dashed lines) in (e) HW/PEI:M, (f) HW/PEI/TA:M, (g) HW/PEI:(A + M), (h) HW/PEI/TA:(A + M). The white arrows mark the general particle orientations. The pressing direction is horizontal to the right.

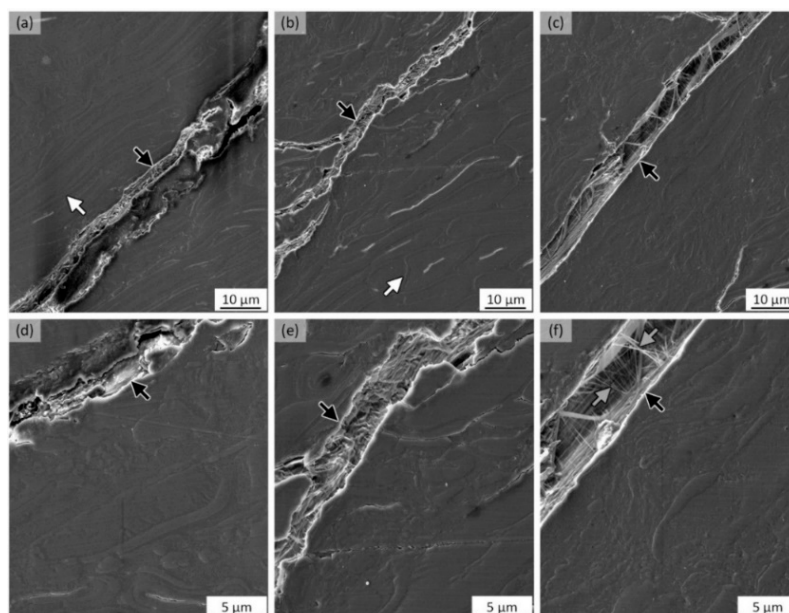


**Figure 5.** SEM microstructures of (a,d) HW/PEI/TA and (b,c,e,f) HW/PEI:(A+M), showing cracks (black arrows) penetrating less deformed cells (white arrows) and severely deformed cells with the pull-out of cellulose fibrils (grey arrows in f). The pressing direction is horizontal to the right.

Figure 6 shows fluorescence overlay images for HW/PEI/TA without or with different pre-treatments, before and after ECAP. Similar to observations in Reference [13], continuous morphologies were formed in all the samples after ECAP. The bright blue fluorescence emission in particles before ECAP significantly diminished (quenching) after ECAP with red or dark color dominating at the edges of particles possibly due to the formation of quinone structures and TA's addition. The dark regions appeared mainly between particles, suggesting that TA was involved in interparticle cross-linking. The samples with ball milling after ECAP (Figure 6f,h) show thinner bright blue cores surrounded by thicker red or dark layers. Ball milling decreased the particle size and crystallinity [14,15] while it increased the specific surface area, causing wood cells and particle structures to become easier to be distorted during ECAP. It also promoted effective binder (PEI and TA) penetration into wood particles, resulting in effective cross-linking and quenching between wood particles and the formation of continuous morphologies. However, shear deformation seemed less homogeneous as most particles still tended to orient at a lower angle ( $<30^\circ$ ) relative to the pressing direction due to less shear interaction between particles when PEI penetration and plasticization effects were enhanced. On the contrary, wood particles without ball milling may have a higher chance of crack formation, although these particles' shear deformation appeared to be more homogeneous. PEI at interparticle surfaces caused more particle rotation towards the shear plane.

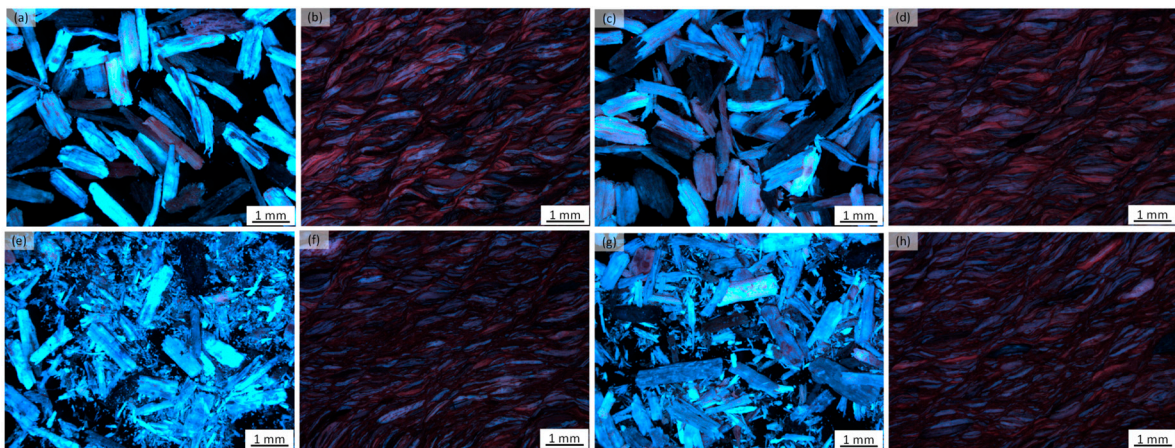


**Figure 6.** Fluorescence overlay images of HW/PEI/TA particles before ECAP (left) and consolidated biocomposites after ECAP (right): (a,b) with no pre-treatment, (c,d) with alkali pre-treatment, (e,f) with ball milling, and (g,h) with alkali + ball milling.

### 3.2. FT-IR Results: Intermolecular Interactions and Crosslinking

The intermolecular interactions in the ECAP processed HW composites were examined by FT-IR. As reported previously [16], the lateral order index (LOI), which indicates the overall degree of order in the cellulose and is related to the crystallinity of cellulose I, is defined as the ratio between the heights of absorbance bands at  $1420\text{--}1430\text{ cm}^{-1}$  and  $893\text{--}898\text{ cm}^{-1}$ . The hydrogen bond intensity (HBI), defined as the band height ratio between  $\sim 3400\text{ cm}^{-1}$  and  $\sim 1320\text{ cm}^{-1}$ , is employed to show the crystallinity and bound water amount [17,18]. The cross-linked lignin ratio (CLL), defined as the ratio between band heights at  $1504\text{ cm}^{-1}$  and  $1590\text{ cm}^{-1}$ , is used to evaluate the percentage of condensed and cross-linked G-type lignin [19,20]. These data for the HW particles without and with pre-treatments are listed in Table 2, showing that ordered cellulose composition slightly increased after alkali treatment but significantly reduced after ball milling. Alkali pre-treatment could cause partial removal of lignin and hemicellulose [14,21], increasing cellulose's relative crystallinity. On the contrary, ball milling would disturb the crystalline structure and reduce the crystallinity [14,15]. The HBI was enhanced after these pre-treatments, while the CLL all decreased due to a reduction in lignin.

**Table 2.** FTIR peak ratios of HW particles without and with different pre-treatments.

Sample	$I_{1422}/I_{896}$ LOI	$I_{3400}/I_{1320}$ HBI	$I_{1504}/I_{1590}$ CLL
HW	1.214	2.849	0.684
HW:A	1.243	3.216	0.613
HW:M	0.884	3.376	0.609
HW:(A + M)	1.010	3.747	0.603

Figure 7 shows FT-IR absorbance spectra of a series of HW samples with different pre-treatments. Like the previous report [13], the formation of strong hydrogen bonding or cross-linking between PEI and  $>C=O$  groups in the wood particles was detected as the increase of the relative peak intensity at  $1650\text{ cm}^{-1}$ . Compared with other as-prepared particles, HW/PEI:A (Figure 7d) shows a higher relative absorbance intensity at  $1565\text{ cm}^{-1}$  before ECAP, indicating less consumption of amino groups. The alkali pre-treatment could have reduced  $>C=O$  groups by deacetylation and removing uronic acid groups in hemicelluloses [14,21], leading to less cross-linking between HW and PEI. After ECAP, the relative intensity at  $1565\text{ cm}^{-1}$  was weakened while the peak at  $1650\text{ cm}^{-1}$  became broad for most HW/PEI and HW/PEI/TA samples, suggesting further consumption of PEI amino groups for cross-linking with HW during ECAP. The smaller decrease in the relative intensity at  $1735\text{ cm}^{-1}$  after ECAP for the alkali pre-treated HW/PEI (HW/PEI:A and HW/PEI:(A + M) in Figure 7d) suggested that the alkali pre-treatment may have reduced the number of  $>C=O$  groups for cross-linking with PEI during ECAP. This caused a smaller decrease in the relative peak intensity at  $1735\text{ cm}^{-1}$ . On the other hand, HW/PEI/TA:A and HW/PEI/TA:(A+M) (Figure 7f) showed a bigger drop at  $1735\text{ cm}^{-1}$  after ECAP. When TA was added to the alkali-treated particles, the  $>C=O$  groups from TA could react with PEI, leading to the drop in intensity at  $1735\text{ cm}^{-1}$  after ECAP. In contrast, for particles without alkali pre-treatment, especially HW/PEI/TA:M, the amount of  $>C=O$  groups would be relatively higher, thereby not showing much further decrease after ECAP.

The amino groups in PEI could form covalent bonds with carbonyl groups in chemical components of wood such as oxidized cellulose and lignin and lead to the formation of conjugated imines with heating [22–24]. With many phenolic hydroxyl groups, TA could also act as a crosslinker by forming covalent bonds with the amino groups in PEI in a similar way as lignin [25,26], resulting in a stronger cross-linking network. The amino groups in PEI and hydroxyl groups in TA and HW components could also form strong hydrogen bonding, contributing to adhesion between wood particles. These results should, therefore, have an impact on the mechanical properties of the HW biocomposites, which would be discussed in the following section.

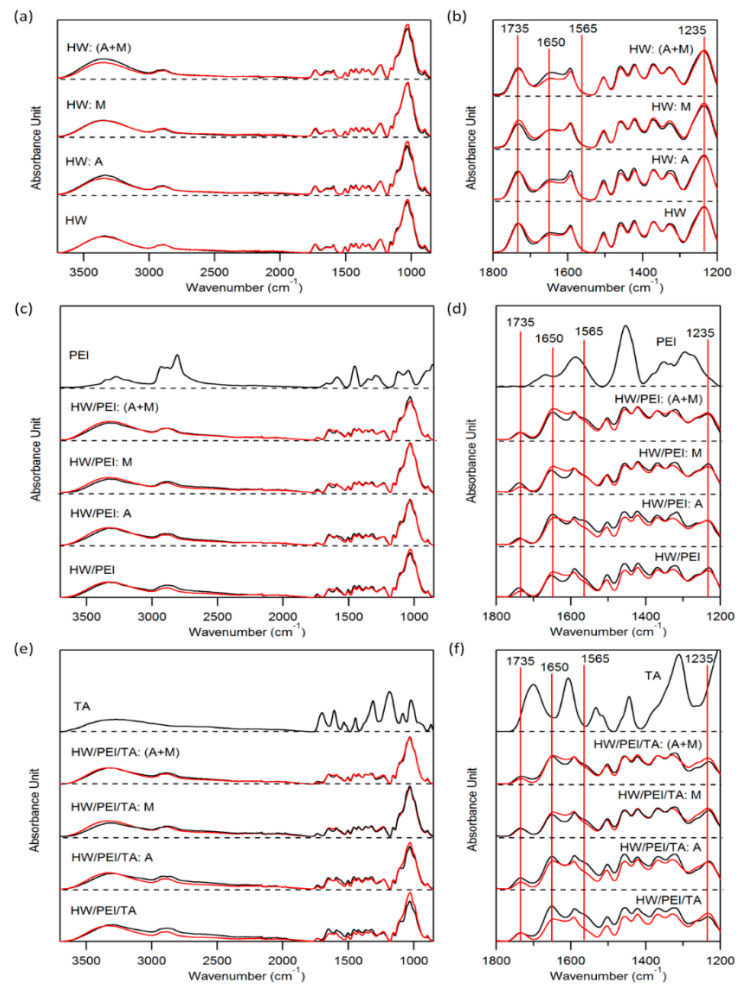


**Figure 7.** FT-IR absorbance spectra for HW, HW/PEI and HW/PEI/TA before (black) and after (red) ECAP.

### 3.3. Mechanical Properties and Thermal Stability

The flexural strength and modulus values of the ECAP processed HW biocomposites are shown in Table 3.

**Table 3.** Flexural strength and modulus results of ECAP consolidated HW biocomposites with different pre-treatments.

Pre-Treatment	HW/PEI = 90/10		HW/PEI/TA = 86/11/3	
	Flexural Strength (MPa)	Flexural Modulus (MPa)	Flexural Strength (MPa)	Flexural Modulus (MPa)
No pre-treatment	15.8 ± 1.7	2836 ± 337	24.6 ± 2.4	3259 ± 358
Alkali	15.2 ± 1.3	2371 ± 297	17.6 ± 2.5	2527 ± 381
Ball milling	19.7 ± 3.3	3786 ± 95	23.3 ± 2.2	3600 ± 247
Alkali + Ball milling	28.1 ± 2.7	3625 ± 272	29.2 ± 4.0	3650 ± 150

Adding TA to the HW/PEI system would increase both flexural strength and modulus, especially for HW without any pre-treatment. However, alkali treatment did not lead to any benefit for HW/PEI. Ball milling only showed positive effects on HW/PEI, but not much on HW/PEI/TA. Applying both alkali and ball milling appeared to have produced the most improvement for both HW/PEI and HW/PEI/TA, with a flexural strength of 28–29 MPa, nearly 20% higher than reported previously without using these pre-treatments and TA additive [7]. The results corroborate the observations in microstructures and

intermolecular interaction/cross-linking studies, demonstrating the benefit of using a combination of alkali and ball milling pre-treatments to improve bonding and consequently mechanical properties of the HW biocomposites.

DMA results in Figure 8 displayed the storage modulus  $E'$  over a broad temperature range. It is noted that most of the samples were brittle, and cracks occurred during the DMA testing. This made it further difficult to distinguish factors from cross-linking and thermo-decomposition, which would be both enhanced at higher temperatures. The  $E'$  decreased slowly with increasing temperature in general; however, no clear glass transition was detected due to the wide distribution of molecular and morphological structures, including cross-linking in these materials. An increase in  $E'$  during a certain heating stage was also observed, possibly owing to stress relief by molecule rearrangements. The sample brittleness was reflected by the low  $\tan\delta$  peaks corresponding to low molecular motions even at high temperatures.

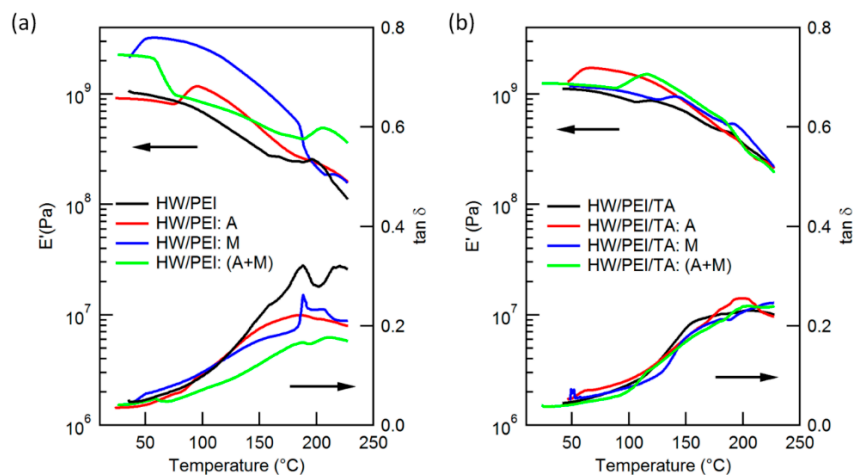


**Figure 8.** Dynamic mechanical analysis (DMA) results of ECAP consolidated (a) HW/PEI and (b) HW/PEI/TA.

Figure 9 shows the TG and DTG curves of TA, HW/PEI and HW/PEI/TA before ECAP, and LF-HW/PEI/TA after ECAP (LF means low friction at the channel walls). TA thermally decomposed at a lower temperature than that for HW/PEI; however, the DTG peak for HW/PEI/TA shifted to higher temperatures compared to that of HW/PEI and TA, further suggesting the possible cross-linking between HW and TA. However, the difference in thermal stability between ECAP consolidated HW/PEI and HW/PEI/TA is minimal, as listed in Table 4. Most of the lignocellulose-based materials would start significant thermo-decompositions above 230 °C, which should be the key factor in considering the application of these bio-composites.

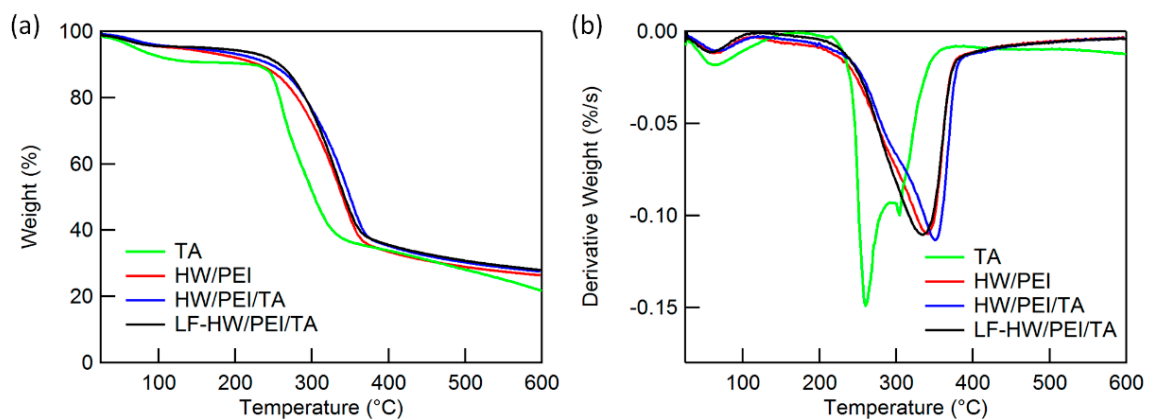


**Figure 9.** Comparison between TA, HW/PEI, HW/PEI/TA and LF-HW/PEI/TA: (a) TG and (b) DTG.

**Table 4.** TGA results of ECAP consolidated HW biocomposites.

Pre-Treatment	HW/PEI = 90/10			HW/PEI/TA = 86/11/3		
	Ti (°C) 10 wt% Loss	DTG Peak (°C)	Residue at 600 °C (%)	Ti (°C) 10 wt% Loss	DTG Peak (°C)	Residue at 600 °C (%)
No treatment	255	331	27.1	258	334	28.0
Alkali	251	333	25.8	258	336	27.4
Ball milling	255	331	26.9	256	334	27.9
Alkali + Ball milling	253	334	26.5	255	333	27.1

#### 4. Conclusions

Following a series of recent research in the area, this work further demonstrated the benefit of using a combination of alkali and ball milling pre-treatments in consolidating HW particles into biocomposites via ECAP. The alkali pre-treatment removed some lignin or hemicellulose from HW particles' surface, generating additional pore structures. Simultaneously, ball milling decreased the particle size and crystallinity of cellulose, facilitating the penetration of bonding additives PEI and TA into HW structures and enhancing plasticization and cross-linking. A significant improvement in mechanical properties was obtained, reaching flexural strength of 28–29 MPa and flexural modulus of >3.6 GPa, comparable with those displayed by commercial particleboard, medium-density fiberboard, or oriented strand board with thermosetting resins as binding materials.

**Author Contributions:** Conceptualization, X.Z. and K.X.; formal analysis, Y.B.; investigation, Y.B.; methodology, Y.B. and K.X.; resources, K.X.; supervision, X.Z. and K.X.; writing—original draft, Y.B.; writing, review and editing, X.Z. and K.X. All authors have read and agreed to the published version of the manuscript.

**Funding:** This research received no external funding.

**Acknowledgments:** We would like to thank Roger Curtain from the Bio 21 Advanced Microscopy Facility (the University of Melbourne), Allison Van De Meene from Biosciences Microscopy Unit, School of Biosciences (the University of Melbourne), Hao Wei from the School of Chemistry (the University of Melbourne), Weidong Yang from CSIRO, and Edward Lui from RMIT University for their valuable assistance with experiments. Y.B. acknowledges financial support from the Research Training Program (RTP) Scholarship and Melbourne Research Scholarship (MRS).

**Conflicts of Interest:** The authors declare no conflict of interest.

#### References

- Narayan, R. Biobased and biodegradable polymer materials: Rationale, drivers, and technology exemplars. In *Degradable Polymers and Materials*; Khemani, K.C., Scholz, C., Eds.; American Chemical Society: Washington, DC, USA, 2006; Volume 939, pp. 282–306.
- Gironi, F.; Piemonte, V. Bioplastics and petroleum-based plastics: Strengths and weaknesses. *Energy Sources Part A Recov. Util. Environ. Eff.* **2011**, *33*, 1949–1959. [[CrossRef](#)]
- Howell, S.G. A ten year review of plastics recycling. *J. Hazard. Mater.* **1992**, *29*, 143–164. [[CrossRef](#)]
- Isikgor, F.H.; Becer, C.R. Lignocellulosic biomass: A sustainable platform for the production of bio-based chemicals and polymers. *Polym. Chem.* **2015**, *6*, 4497–4559. [[CrossRef](#)]
- Stokke, D.D.; Wu, Q.; Han, G. *Introduction to Wood and Natural Fiber Composites*; John Wiley & Sons: Chichester, UK, 2014.
- Witkowski, A.; Stec, A.A.; Hull, T.R. Thermal decomposition of polymeric materials. In *SFPE Handbook of Fire Protection Engineering*, 5th ed.; Hurley, M.J., Gottuk, D., Hall, J.R., Harada, K., Kuligowski, E., Puchovsky, M., Torero, J., Watts, J.M., Wieczorek, C., Eds.; Springer: New York, NY, USA, 2016; pp. 167–254. [[CrossRef](#)]
- Rowell, R.M. *Handbook of Wood Chemistry and Wood Composites*, 2nd ed.; CRC Press: Boca Raton, FL, USA, 2012.
- Navi, P.; Sandberg, D. Wood densification and fixation of the compression-set by THM treatment. In *Thermo-Hydro-Mechanical Wood Processing*; Navi, P., Sandberg, D., Eds.; EPFL Press: Boca Raton, FL, USA, 2012; pp. 193–224.

9. Zhang, X.; Gao, D.; Wu, X.; Xia, K. Bulk plastic materials obtained from processing raw powders of renewable natural polymers via back pressure equal channel angular consolidation (BP-ECAC). *Eur. Polym. J.* **2008**, *44*, 780–792. [[CrossRef](#)]
10. Zhang, X.; Wu, X.; Gao, D.; Xia, K. Bulk cellulose plastic materials from processing cellulose powder using back pressure-equal channel angular pressing. *Carbohydr. Polym.* **2012**, *87*, 2470–2476. [[CrossRef](#)]
11. Zhang, X.; Wu, X.; Xia, K. Cellulose-wheat gluten bulk plastic materials produced from processing raw powders by severe shear deformation. *Carbohydr. Polym.* **2013**, *92*, 2206–2211. [[CrossRef](#)]
12. Zhang, X.; Wu, X.; Haryono, H.; Xia, K. Natural polymer biocomposites produced from processing raw wood flour by severe shear deformation. *Carbohydr. Polym.* **2014**, *113*, 46–52. [[CrossRef](#)]
13. Bai, Y.; Zhang, X.; Xia, K. High strength biocomposites consolidated from hardwood particles by severe plastic deformation. *Cellulose* **2019**, *26*, 1067–1084. [[CrossRef](#)]
14. Hendriks, A.T.W.M.; Zeeman, G. Pretreatments to enhance the digestibility of lignocellulosic biomass. *Bioresour. Technol.* **2009**, *100*, 10–18. [[CrossRef](#)]
15. Karinkanta, P.; Ämmälä, A.; Illikainen, M.; Niinimäki, J. Fine grinding of wood—Overview from wood breakage to applications. *Biomass Bioenergy* **2018**, *113*, 31–44. [[CrossRef](#)]
16. O'Connor, R.T.; DuPré, E.F.; Mitcham, D. Applications of infrared absorption spectroscopy to investigations of cotton and modified cottons: Part I: Physical and crystalline modifications and oxidation. *Text. Res. J.* **1958**, *28*, 382–392. [[CrossRef](#)]
17. Nada, A.-A.M.A.; Kamel, S.; El-Sakhawy, M. Thermal behaviour and infrared spectroscopy of cellulose carbamates. *Polym. Degrad. Stab.* **2000**, *70*, 347–355. [[CrossRef](#)]
18. Oh, S.Y.; Yoo, D.I.; Shin, Y.; Seo, G. FTIR analysis of cellulose treated with sodium hydroxide and carbon dioxide. *Carbohydr. Res.* **2005**, *340*, 417–428. [[CrossRef](#)]
19. Auxenfans, T.; Crônier, D.; Chabbert, B.; Paës, G. Understanding the structural and chemical changes of plant biomass following steam explosion pretreatment. *Biotechnol. Biofuels* **2017**, *10*. [[CrossRef](#)] [[PubMed](#)]
20. Mann, D.G.J.; Labbé, N.; Sykes, R.W.; Gracom, K.; Kline, L.; Swamidoss, I.M.; Burriss, J.N.; Davis, M.; Stewart, C.N. Rapid assessment of lignin content and structure in switchgrass (*Panicum virgatum* L.) grown under different environmental conditions. *Bioenergy Res.* **2009**, *2*, 246–256. [[CrossRef](#)]
21. Mosier, N.; Wyman, C.; Dale, B.; Elander, R.; Lee, Y.Y.; Holtzapple, M.; Ladisch, M. Features of promising technologies for pretreatment of lignocellulosic biomass. *Bioresour. Technol.* **2005**, *96*, 673–686. [[CrossRef](#)] [[PubMed](#)]
22. Martínez Urreaga, J.; de la Orden, M.U. Modification of cellulose with amino compounds: A fluorescence study. *Carbohydr. Polym.* **2007**, *69*, 14–19. [[CrossRef](#)]
23. Faris, A.H.; Rahim, A.A.; Ibrahim, M.N.M.; Alkurdi, A.M.; Shah, I. Combination of lignin polyol–tannin adhesives and polyethylenimine for the preparation of green water-resistant adhesives. *J. Appl. Polym. Sci.* **2016**, *133*. [[CrossRef](#)]
24. Geng, X.; Li, K. Investigation of wood adhesives from kraft lignin and polyethylenimine. *J. Adhes. Sci. Technol.* **2006**, *20*, 847–858. [[CrossRef](#)]
25. Zhang, X.; Do, M.D.; Casey, P.; Sulistio, A.; Qiao, G.G.; Lundin, L.; Lillford, P.; Kosaraju, S. Chemical cross-linking gelatin with natural phenolic compounds as studied by high-resolution NMR spectroscopy. *Biomacromolecules* **2010**, *11*, 1125–1132. [[CrossRef](#)]
26. Li, K.; Geng, X.; Simonsen, J.; Karchesy, J. Novel wood adhesives from condensed tannins and polyethylenimine. *Int. J. Adhes. Adhes.* **2004**, *24*, 327–333. [[CrossRef](#)]

**Publisher's Note:** MDPI stays neutral with regard to jurisdictional claims in published maps and institutional affiliations.



© 2020 by the authors. Licensee MDPI, Basel, Switzerland. This article is an open access article distributed under the terms and conditions of the Creative Commons Attribution (CC BY) license (<http://creativecommons.org/licenses/by/4.0/>).